ORIGINAL PAPERS

**Lin-gun Liu · Chien-chih Chen · Chung-Cherng Lin
Yi-jong Yang**

Elasticity of single-crystal aragonite by Brillouin spectroscopy

Abstract The elastic constants of natural single-crystal aragonite ($CaCO_3$) have been measured by Brillouin spectroscopy at ambient conditions. The elastic constants C_{11}, C_{22}, C_{33}, C_{44}, C_{55}, C_{66}, C_{12}, C_{13} and C_{23} are 171.1 ± 1.0, 110.1 ± 0.9, 98.4 ± 1.2, 39.3 ± 0.6, 24.2 ± 0.4, 40.2 ± 0.6, 60.3 ± 1.0, 27.8 ± 1.6 and 41.9 ± 2.0 GPa, respectively, for aragonite. The linear compressibilities of the a-, b- and c-axis for aragonite at ambient conditions were derived from our measured data to be 3.0 ± 0.2, 4.2 ± 0.2 and $7.3 \pm 0.6 \times 10^{-3}$ GPa^{-1}, respectively. The aggregate bulk and shear moduli for aragonite using the Voigt-Reuss-Hill (VRH) scheme are thus calculated to be 68.9 ± 1.4 and 35.8 ± 0.2 GPa, respectively. The value of bulk modulus is in remarkable contrast to the literature value of 46.9 GPa measured almost a century ago. Our new datum, however, is closer to that derived from recent atomistic simulation and static compression studies.

Keywords Aragonite · Brillouin scattering · Elastic constants

Introduction

For polymorphs undergoing high-pressure transition, it is required by thermodynamics that the phase at high pressure be denser than its adjacent phase at low pressure. It is also conventional wisdom that the bulk modulus for the high-pressure polymorph (or the dense phase) should be greater than that for the corresponding low-pressure polymorph (or the light phase). However, there exist several exceptions that act contrary to the latter rule, e.g., $CaCO_3$, V_3O_5, KCl, ... as revealed from the tables compiled by Bass (1995) and Knittle (1995). On the other hand, most of these exceptions may be artifacts because the bulk moduli of these materials were derived from volume compression studies. Only the values of bulk modulus for the pair of calcite and aragonite (both are $CaCO_3$) were derived from measured elastic constants. The bulk modulus for calcite is about 60% greater than that for aragonite (76 GPa vs. 47 GPa), yet aragonite is about 8% denser than calcite. It appears that the value of bulk modulus for calcite is likely to be more reliable than that for aragonite because the elastic constants for calcite have been measured several times (e.g., Chen et al. 2001; and many references cited therein), whereas those for aragonite have been measured only once, about a century ago (Voigt 1910). On the other hand, elasticity of aragonite has been studied by e.g., Pavese et al. (1992) and Fisler et al. (2000) using theoretical models. We attempt to re-measure the elasticity of aragonite by Brillouin spectroscopy in the present study.

Samples and experimental procedures

Samples

As mentioned earlier, the elastic constants of aragonite have been measured only once, by Voigt (1910) using an ultrasonic technique. Through the present study, we realized the difficulties involved in measuring the elastic constants of aragonite employing the ultrasonic techniques, because most natural samples of aragonite are porous and contaminated by impurities. Tiny and small voids are particularly common in all the samples so far examined in this study (more than ten different samples from all different localities). Thus, it would be difficult to find big and clear samples for ultrasonic measurements.

L. Liu (✉) · C. Chen · C.-C. Lin · Y. Yang
Institute of Earth Sciences,
Academia Sinica, Nankang,
Taipei, Taiwan, 115, ROC

Present address: C. Chen
Department of Earth Sciences and Institute of Geophysics,
National Central University, Chungli,
Taiwan, 320, ROC

Carbonates	wt%
$CaCO_3$	97.4
$SrCO_3$	2.5
$MgCO_3$	< 0.1
$MnCO_3$	< 0.1
$FeCO_3$	< 0.1

For Brillouin spectroscopy study, the sample size can be reduced to a few mm or even a few tens of μm (e.g., Liu et al. 2004). The samples used in the present work (from Penhu, Taiwan) are optically clear natural single crystals without twining and are approximately 2×3 mm^2 $\times 80$ μm in size. Chemical composition of the sample analyzed by an electron probe is as follows:

Powder and single-crystal X-ray diffraction studies confirmed the sample to be aragonite, and the lattice parameters are $a_0 = 4.951 \pm 0.001$, $b_0 = 7.963 \pm 0.014$, and $c_0 = 5.733 \pm 0.001$ Å. These parameters are in good agreement with those in the JCPDS card (5–453).

Brillouin scattering measurements

Four platelets of aragonite have been employed in the present experiment. The two opposite sides of these platelets were finely polished to about 80 μm and were parallel to each other within ± 10'. Brillouin spectra were also collected with the two sides of the platelet reversed to reduce possible errors introduced by non-parallelism of the platelet faces.

Each platelet was then mounted on an Eulerian cradle, which was used to control the sample orientation on the Brillouin system. An argon ion laser ($\lambda = 514.5$ nm) with 100 mW of power and a six-pass tandem Fabry-Pérot interferometer were used for the Brillouin experiments. Our Brillouin experiment utilizes a symmetric scattering geometry with an external angle between the incident and scattered beams of 90°, which yields acoustic velocity measurements independent of the refractive index of the specimen, and the Brillouin frequency shift, $\Delta\omega$, is directly related to the acoustic velocity V and the incident laser wavelength λ by

$$V = \Delta\omega\lambda/\sqrt{2}. \tag{1}$$

A Brillouin spectrum consists of an elastically scattered component with the same frequency as the excitation source and a set of inelastically scattered components. The latter displays a frequency shift caused by the interaction between photons and phonons in the sample. Details of the Brillouin scattering technique have been widely elucidated in literature (e.g., Sinogeikin and Bass 2000; Chen et al. 2001).

The birefringence of anisotropic crystals can be problematic when utilizing Eq. 1, because birefringence can yield double peaks or cause peak broadening in the Brillouin spectrum. It can be expected that the problem for aragonite should be much less than that for calcite and rhodochrosite because the birefringences for the latter two carbonates are much higher than that for aragonite. We have previously measured elasticity of calcite and rhodochrosite using the same experimental technique (Chen et al. 2001). Thus, as can be expected, the Brillouin peaks of aragonite would be generally sharp (see Fig. 1), and the possible errors introduced by the birefringence of aragonite are minor. The details of this issue have also been elucidated earlier (Sinogeikin and Bass 2000; Chen et al. 2001).

The measured acoustic velocities of a series of co-planer orientations are illustrated in Fig. 2 for the four platelets of aragonite. The final data set of aragonite for elasticity inversion consisted of 187 mode velocity determinations (Fig. 2), and all of these are averages of three or more redundant measurements in each direction to ensure the reproducibility of the Brillouin data.

Phonon direction analysis and inversion of C_{ij}

Aragonite is orthorhombic and requires nine elastic constants to completely describe its elastic properties. It has been demonstrated by Duffy et al. (1995) and Zha et al. (1997) that it is possible to deduce the complete set of the nine elastic constants by measuring in a single crystallographic plane of an orthorhombic crystal. For non-cubic crystals, however, collecting data in at least two orthogonal planes could minimize co-variance be-
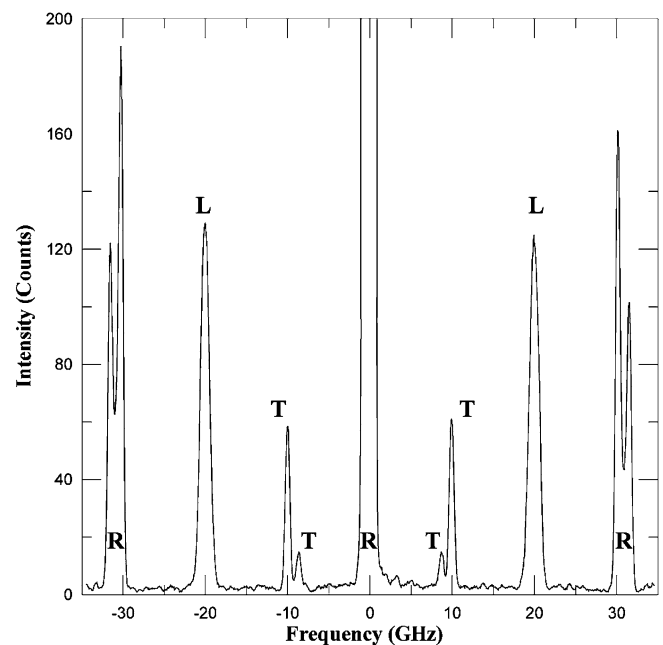
Fig. 1 A representative Brillouin spectrum of aragonite. L and T indicate the longitudinal and transverse modes, respectively, and R the Rayleigh peaks. The spectrum was collected in a phonon direction of (−0.743, 0.669, 0.000) on the plane having a normal vector of (0, 0, 1) at a χ angle of 180 degrees (see Fig. 2a)

Fig. 2 Observed and calculated longitudinal (*semi filled diamond* and *dotted lines*) and transverse (*circled plus* and blue lines for the first mode; *open square* and *red lines* for the second mode) acoustic velocities as a function of χ angle, which is about an arbitrary setting mark on the three-circle Eulerian cradle, for the four platelets of aragonite used in this study. The *fitted lines* were calculated from the best-fitting elastic constants listed in Table 1. Normal vectors and specific phonon directions relative to the Cartesian system for each crystallographic plane are also shown, together with the root-mean-square deviations between calculated and measured velocities
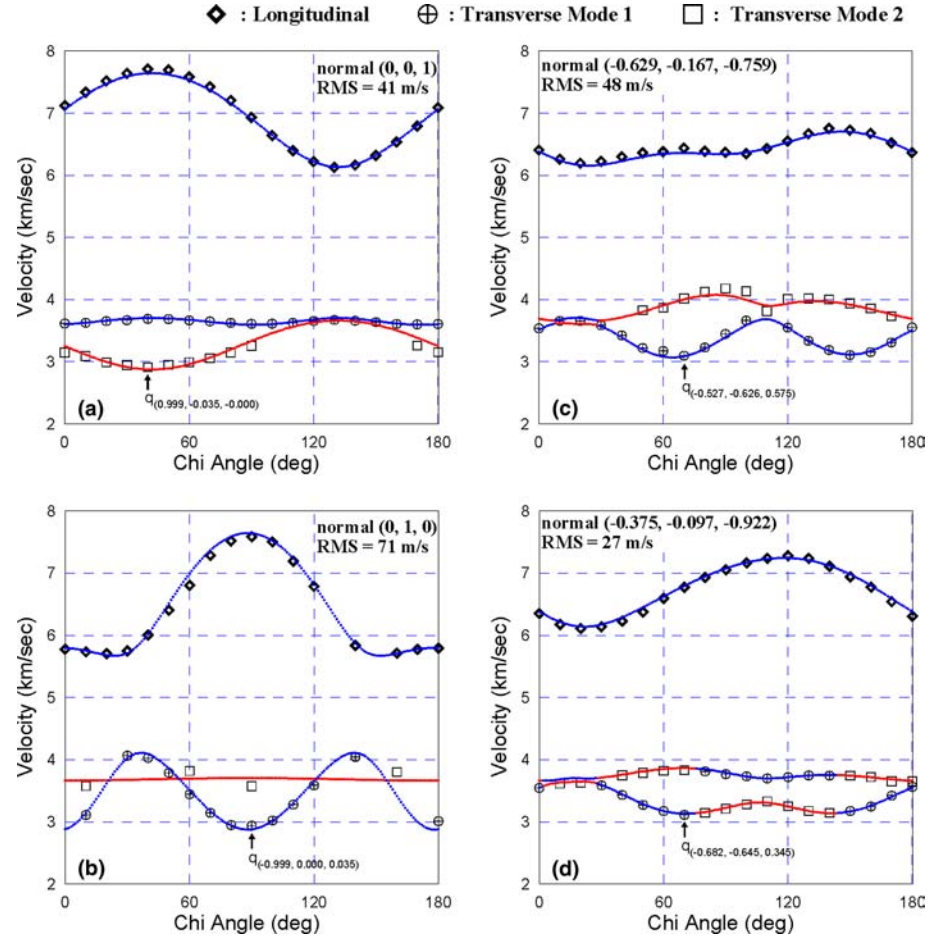
tween the values of C_{ij}, and thus provides the most accurate set of the elastic constants.

Two of the platelets of our samples were cut perpendicular to the orthogonal [010] and [001] axes. The orientations of these two platelets were also confirmed by single-crystal X-ray diffraction. A least-square algorithm was then used to calculate the phonon directions of the observed velocities with inputs of the known normal vectors of these two crystallographic planes. For the other two platelets with unknown orientation, a reasonable set of elastic constants was first assumed and then the observed velocity data were used to calculate the normal vectors of the planes by a least-squares algorithm. The accuracy of orientation thus determined was estimated to be < ±2° by Sinogeikin and Bass (2000). After a series of iterations, the normal vectors for these two platelets were determined to be (−0.375, −0.097, −0.922) and (−0.629, −0.167, −0.759). The independence of the four crystallographic planes ensures the reliability of our measurement for the elastic constants of aragonite.

In putting the velocity data together with the fitted phonon directions, we used a nonlinear inversion procedure to solve the nine elastic constants of aragonite. The nonlinear inversion procedure uses the Gauss–Newton algorithm with Levenberg–Marquardt modifications for global convergence of solutions, and has been adopted widely in finding solutions to the Christoffel equations (e.g., Zha et al. 1996). Although it is possible that the effect of uncertainties in the phonon directions could be amplified in solving the elastic constants (Every 1980), the final estimation for both the phonon directions and the elastic constants indeed converged toward a reliable result in this study, after iterating the above two steps several times.

Results and discussion

The elastic constants of orthorhombic aragonite obtained in this study are listed in Table 1, together with Voigt's data and theoretical estimates (Pavese et al. 1992; Fisler et al. 2000). The C_{ij} of calcite from our earlier measurement (Chen et al. 2001) are also included in Table 1 for comparison.

The data of the present measurement of aragonite show major differences in the off-diagonal C_{ij} with Voigt's data, but are in better agreement with those calculated by Pavese et al. (1992) and Fisler et al. (2000). It should be emphasized that the theoretical works did not actually predict the elastic constants but fit them, except that they gave the null weighting for the three off-

Table 1 Elastic constants (C_{ij}, in GPa) of aragonite and calcite and the calculated and experimental axial compressibilities ($\beta_x = -1000d(x/x_0)/dP$, $x = a, b, c$, and P in GPa) of aragonite. Bulk/shear modulus K/G, in GPa

	Aragonite							Calcite[a]
	Experimental data			Model values				
	This work	Voigt (1910)	Martinez et al. (1996)	Fisler et al. (2000)	Pavese et al. (1992)			Chen et al. (2001)
					RIM 1	RIM 2	RIM	
C_{11}	171.1 ± 1.0	159.6		155.3	164.4	157.7	194.2	149.4
C_{22}	110.1 ± 0.9	87.0		104.2	112.0	100.9	117.1	149.4
C_{33}	98.4 ± 1.2	85.0		89.9	59.2	68.3	71.3	85.2
C_{44}	39.3 ± 0.6	41.3		36.7	40.5	36.0	44.1	34.1
C_{55}	24.2 ± 0.4	25.6		12.4	33.9	24.1	34.5	34.1
C_{66}	40.2 ± 0.6	42.7		23.3	49.0	41.1	43.8	45.8
C_{12}	60.3 ± 1.0	36.6		55.9	65.3	58.0	65.9	57.9
C_{13}	27.8 ± 1.6	2.0		54.7	39.0	34.1	35.7	53.5
C_{23}	41.9 ± 2.0	15.9		48.0	48.2	50.4	50.2	53.5
β_a	3.0 ± 0.2	4.3	$3.0 (2.4)^b$	2.1	2.1	3.0	2.3	
β_b	4.6 ± 0.2	7.8	$4.2 (4.2)^b$	5.2	1.6	2.6	2.5	
β_c	7.3 ± 0.6	10.2	$6.5 (5.8)^b$	7.1	14.2	11.3	11.1	
K_{VRH}	68.9 ± 1.4	46.9	$73.0^c (80.6)^c$	71.8	63.5	63.8	69.6	76.1
G_{VRH}	35.8 ± 0.2	38.5		25.0	33.8	30.1	37.2	32.8

[a] $C_{14} = -20$ and $C_{66} = (C_{11}-C_{12})/2$
[b] The values inside the parentheses are from Martinez et al. (1996) and those without parentheses are derived in this study (see Fig. 3 and text for details).
[c] These values of bulk modulus were derived from Eq. 2 using the compression data of β_a, β_b, and β_c

diagonal C_{12}, C_{13} and C_{23} constants in the fitting. As argued by Pavese et al. (1992), the very old experimental values for the off-diagonal terms might be affected by significant errors in measurements. Our new data of C_{ij} for aragonite are thus helpful to judge the atomistic models used by Pavese et al. (1992) and Fisler et al. (2000). Table 1 also shows that Voigt's off-diagonal elements for aragonite are much smaller than the corresponding ones for calcite. This appears unreasonable from the viewpoint of theoretical models (Pavese et al. 1992; Fisler et al. 2000). The off-diagonal elements for aragonite obtained in the present work come to much closer to those for calcite.

The elastic constants of aragonite determined from Brillouin data can also be directly compared with that of the linear compressibility measured by X-ray diffraction study of Martinez et al. (1996), who have reported that the linear compressibilities of the a-, b- and c-axis for aragonite at room temperature are 2.4 ± 0.2, 4.2 ± 0.2 and $5.8 \pm 0.2 \times 10^{-3}$ GPa^{-1}, respectively (see β_a, β_b, and β_c in Table 1). However, the raw data of their study were reported in both a table and a figure, but the number of data are not consistent to each other. There are three extra data points at about 1.1, 2.3 and 5.5 GPa for all three axes in the figure. Thus, it is not certain that the linear compressibilities reported by them were derived from the data shown in the table or the figure. Because one cannot accurately read the data displayed in a figure, only the 298-K data reported in their table are shown in Fig. 3. Except for the initial point, Martinez et al. (1996) listed two 298-K data points at each pressure. According to these authors, one set of the data was obtained using calcite as the starting material and the other set of data was obtained using aragonite. In order to avoid possible complications, only the data obtained using aragonite starting material are shown in Fig. 3. The linear compressibilities of the a-, b- and c-axis for aragonite derived from the data shown in Fig. 3 are 3.0 ± 0.2, 4.2 ± 0.2 and $5.5 \pm 0.2 \times 10^{-3}$ GPa^{-1}, respectively, fitting the data to linear regressions (the solid lines in Fig. 3). The linear compressibility of the a-axis (or β_a) thus calculated is significantly greater than that reported by Martinez et al. (1996). Figure 3 also shows that the compression of the c-axis may not be linear. This is particularly obvious for the c-axis data shown in the figure of Martinez et al. (1996). By fitting the c-axis data of Fig. 3 to a quadratic regression (the dashed line in Fig. 3), the initial slope of the linear compressibility of the c-axis is $6.5 \pm 0.2 \times 10^{-3}$ GPa^{-1}, which is also significantly greater than that derived earlier. Thus, it demonstrates that the reported values of linear compressibilities for aragonite are subjected to much greater uncertainties than one would like to admit. By definition, the following relationship must be held for an orthorhombic crystal

$$\beta = \beta_a + \beta_b + \beta_c, \qquad (2)$$

where β is the volume compressibility. Following Eq. 2, one should never fit the compression data for all three axes of an orthorhombic crystal to linear regressions. This will yield the consequence that the volume compressibility (or bulk modulus) is independent of pressure.

According to Nye (1957), the linear compressibilities of the orthorhombic axes under hydrostatic pressure are related to the elastic compliances s_{ij}, or the inverse of elastic constants, as follows:
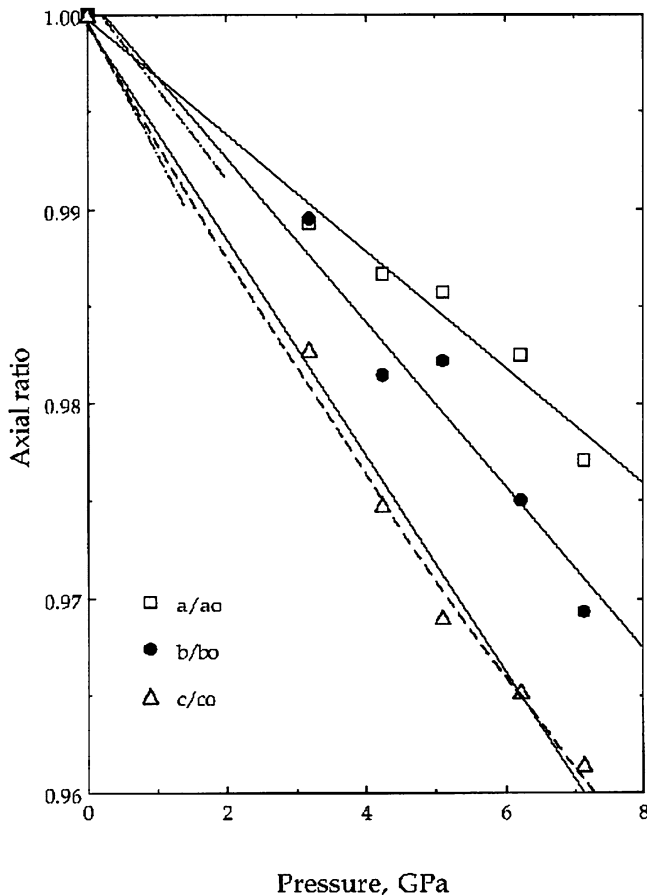
Fig. 3 Variation of a/a_o, b/b_o and c/c_o with pressure at room temperature (data are from Martinez et al. 1996). The *solid lines* are linear regressions to the data, and the *dashed line* is a quadratic regression to the c/c_o data. The *chain lines* are the results of our study derived from Eq. 3

$$d(a/a_0)/dP = s_{11} + s_{12} + s_{13}, \qquad (3.1)$$

$$d(b/b_0)/dP = s_{12} + s_{22} + s_{23}, \qquad (3.2)$$

$$d(c/c_0)/dP = s_{13} + s_{23} + s_{33}. \qquad (3.3)$$

Table 1 shows that the linear compressibilities for aragonite calculated from the elastic constants of the present study via Eq. 3 are in much better agreement with those of the compression data recalculated in the present study. The values of the linear compressibilities for the a- and c-axis reported by Martinez et al. (1996) are both significantly too small. The results of our study derived from Eq. 3 are also shown by chain lines for the b- and c-axis in Fig. 3 (the data for the a-axis are superimposed with that of Martinez et al.) for comparison. For theoretical models, only the a-axis for the RIM2 model of Pavese et al. (1992) and the c-axis of Fisler et al. (2000) are in good agreement with experimental measurements and all others are not in agreement.

The aggregate bulk and shear moduli using the Voigt-Reuss-Hill (VRH) averaging scheme are calculated to be

68.9 ± 1.4 and 35.8 ± 0.2 GPa, respectively, for aragonite from the present work. The value of bulk modulus is significantly greater than that (46.9 GPa) calculated from Voigt's data. The latter is likely to be suffered from voids contaminated in the sample used. As shown in Table 1, the bulk modulus for aragonite of the present study is about 10% smaller than that for calcite (76.1 GPa). In other words, aragonite is more compressible than calcite, though the former is about 8% denser than the latter. As mentioned in the introduction, this is the only exception in which the elasticity for both polymorphs has been well determined. Thus, one may be puzzled whether the samples used in the present study are still suffered by minute voids that were not revealed by our optical microscope. It is also noted, in Table 1, that the bulk moduli of aragonite derived from compression data via Eq. 2 are either comparable or slightly greater than that of calcite. It should be pointed out, however, that the value of 80.6 ± 8.2 GPa for aragonite must be in error, because the reported values of β_a, β_b, and β_c were all derived using linear regressions.

References

Bass JD (1995) Elasticity of minerals, glasses, and melts. In: Ahrens TJ (ed) Mineral physics and crystallography: a handbook of physical constants. American Geophysical Union, Washington, pp 45–63

Chen CC, Lin CC, Liu L, Sinogeikin SV, Bass JD (2001) Elasticity of single-crystal calcite and rhodochrosite by Brillouin spectroscopy. Am Mineral 86:1525–1529

Duffy TS, Zha CS, Downs RT, Mao HK, Hemley RJ (1995) Elasticity of forsterite to 16 GPa and the composition of the upper mantle. Nature 378:170–173

Every AG (1980) General closed-form expressions for acoustic waves in elastically anisotropic solids. Physi Rev B 22:1746–1760

Fisler DK, Gale JD, Cygan RT (2000) A shell model for the simulation of rhombohedral carbonate minerals and their point defects. Am Mineral 85:217–224

Knittle E (1995) Static compression measurements of equation of state. In: Ahrens TJ (ed) Mineral physics and crystallography: a handbook of physical constants. American Geophysical Union, Washington, pp 98–142

Liu L, Okamoto K, Yang Y, Chen C-C, Lin C-C (2004) Elasticity of single-crystal phase D (a dense hydrous magnesium silicate) by Brillouin spectroscopy. Solid State Commun 132:517–520

Martinez I, Zhang J, Reeder RJ (1996) In situ X-ray diffraction of aragonite and dolomite at high pressure and high temperature: evidence for dolomite breakdown to aragonite and magnesite. Am Mineral 81:611–624

Nye JF (1957) Physical Properties of Crystals. Oxford University Press, London, pp 322

Pavese A, Catti M, Price GD, Jackson RA (1992) Interatomic potentials for CaCO$_3$ polymorphs (calcite and aragonite), fitted to elastic and vibrational data. Phys Chem Minerals 19:80–87

Sinogeikin SV, Bass JD (2000) Single-crystal elasticity of pyrope and MgO to 20 GPa by Brillouin scattering in the diamond cell. Phys Earth Planet Inter 120:43–62

Voigt W (1910) Lehrbuch der Kristallphysik, reprinted 1928. Teubner, Leipzig

Watt JP (1987) Polyxstal: a FORTRAN program to calculate average elastic properties of minerals from single-crystal elasticity data. Comput Geosci 13:441–462

Zha CS, Duffy TS, Downs RT, Mao HK, Hemley RJ (1996) Sound velocity and elasticity of single-crystal forsterite to 16 GPa. J Geophys Res 101:17535–17545

Zha CS, Duffy TS, Mao HK, Downs RT, Hemley RJ, Weidner DJ (1997) Single-crystal elasticity of β-Mg_2SiO_4 to the pressure of the 410 km seismic discontinuity in the Earth's mantle. Earth Planet Sci Lett 147:E9–E15